

and, for a short period of time, with one other species group. Skin swab specimens from all other contacted amphibians at the zoos tested negative for *Brucella*. Diet consisted of a variety of insect species, making 2 separate introductions of *Brucella* from an outside source possible but unlikely. These findings highlight the need for additional testing of atypical *Brucella* spp., a potential emerging disease in amphibians, and warrants precautions when handling amphibians because of the potential for zoonoses.

### Acknowledgments

We thank the staff at the Binder Park and John Ball Zoo and Amy Hill, Victoria Watson, and Michelle Magagna.

### About the Author

Dr. Glabman is a veterinary anatomic pathologist and PhD candidate at the National Cancer Institute, Center for Cancer Research, at the National Institutes of Health in Bethesda, Maryland, in partnership with Michigan State University. Her primary research interests include comparative and investigative pathology of human and animal models of disease.

### References

1. Al Dahouk S, Köhler S, Occhialini A, Jiménez de Bagüés MP, Hammerl JA, Eisenberg T, et al. *Brucella* spp. of amphibians comprise genomically diverse motile strains competent for replication in macrophages and survival in mammalian hosts. *Sci Rep*. 2017;7:44420. <https://doi.org/10.1038/srep44420>
2. Fischer D, Lorenz N, Heuser W, Kämpfer P, Scholz HC, Lierz M. Abscesses associated with a *Brucella inopinata*-like bacterium in a big-eyed tree frog (*Leptopelis vermiculatus*). *J Zoo Wildl Med*. 2012;43:625–8. <https://doi.org/10.1638/2011-0005R2.1>
3. Eisenberg T, Hamann HP, Kaim U, Schlez K, Seeger H, Schauerte N, et al. Isolation of potentially novel *Brucella* spp. from frogs. *Appl Environ Microbiol*. 2012;78:3753–5. <https://doi.org/10.1128/AEM.07509-11>
4. Whatmore AM, Dale E, Stubberfield E, Muchowski J, Koylass M, Dawson C, et al. Isolation of *Brucella* from a White's tree frog (*Litoria caerulea*). *JMM Case Rep*. 2015;2:1–5. <https://doi.org/10.1099/jmmcr.0.000017>
5. Soler-Lloréns PF, Quance CR, Lawhon SD, Stuber TP, Edwards JF, Ficht TA, et al. A *Brucella* spp. isolate from a Pac-Man frog (*Ceratophrys ornata*) reveals characteristics departing from classical *Brucellae*. *Front Cell Infect Microbiol*. 2016;6:116. <https://doi.org/10.3389/fcimb.2016.00116>
6. Scholz HC, Mühlendorfer K, Shilton C, Benedict S, Whatmore AM, Blom J, et al. The change of a medically important genus: worldwide occurrence of genetically diverse novel *Brucella* species in exotic frogs. *PLoS One*. 2016;11:e0168872. <https://doi.org/10.1371/journal.pone.0168872>
7. Shilton CM, Brown GP, Benedict S, Shine R. Spinal arthropathy associated with *Ochrobactrum anthropi* in free-ranging cane toads (*Chaunus [Bufo] marinus*) in Australia. *Vet Pathol*. 2008;45:85–94. <https://doi.org/10.1354/vp.45-1-85>
8. Helmick KE, Garner MM, Rhyon J, Bradway D. Clinicopathologic features of infection with novel *Brucella* organisms in captive waxy tree frogs (*Phyllomedusa sauvagii*) and Colorado river toads (*Incilius alvarius*). *J Zoo Wildl Med*. 2018;49:153–61. <https://doi.org/10.1638/2017-0026R1.1>
9. Mühlendorfer K, Wibbelt G, Szentiks CA, Fischer D, Scholz HC, Zschöck M, et al. The role of 'atypical' *Brucella* in amphibians: are we facing novel emerging pathogens? *J Appl Microbiol*. 2017;122:40–53. <https://doi.org/10.1111/jam.13326>
10. De BK, Stauffer L, Koylass MS, Sharp SE, Gee JE, Helsel LO, et al. Novel *Brucella* strain (BO1) associated with a prosthetic breast implant infection. *J Clin Microbiol*. 2008;46:43–9. <https://doi.org/10.1128/JCM.01494-07>

Address for correspondence: Dalen Agnew, Michigan State University Veterinary Diagnostic Laboratory, 4125 Beaumont Road, Lansing, MI 48910; email: [agnewd@msu.edu](mailto:agnewd@msu.edu)

## Incursion of Novel Highly Pathogenic Avian Influenza A(H5N8) Virus, the Netherlands, October 2020

Nancy Beerens, Rene Heutink, Frank Harders, Marit Roose, Sylvia B.E. Pritz-Verschuren, Evelien A. Germeraad, Marc Engelsma

Author affiliation: Wageningen Bioveterinary Research, Lelystad, the Netherlands

DOI: <https://doi.org/10.3201/eid2706.204464>

Highly pathogenic avian influenza A(H5N8) virus was detected in mute swans in the Netherlands during October 2020. The virus shares a common ancestor with clade 2.3.4.4b viruses detected in Egypt during 2018–2019 and has similar genetic composition. The virus is not directly related to H5N8 viruses from Europe detected in the first half of 2020.

**I**ntroduction of highly pathogenic avian influenza (HPAI) H5 clade 2.3.4.4 viruses in Europe caused substantial losses to the poultry industry during 2014–2020. Migratory waterfowl are impli-

cated in the distribution of HPAI H5 viruses along flyways from breeding grounds in northern Russia to wintering sites in Europe (1–3). During 2016, clade 2.3.4.4b HPAI H5N8 viruses were introduced in Europe (4,5) and the Netherlands (6,7). More recent introductions of these viruses were detected in eastern Europe, Germany, and Bulgaria in the first half of 2020 (8,9).

On October 17, 2020, two mute swans (*Cygnus olor*) were found dead in the province of Utrecht, the Netherlands. The swans were diagnostically tested as part of the wild bird surveillance program for avian influenza virus. Swab samples from the trachea and cloaca were PCR-positive for avian influenza virus. The virus was subtyped as HPAI H5N8 and contained the hemagglutinin (HA) cleavage site sequence PLREKRRKR\*GLF.

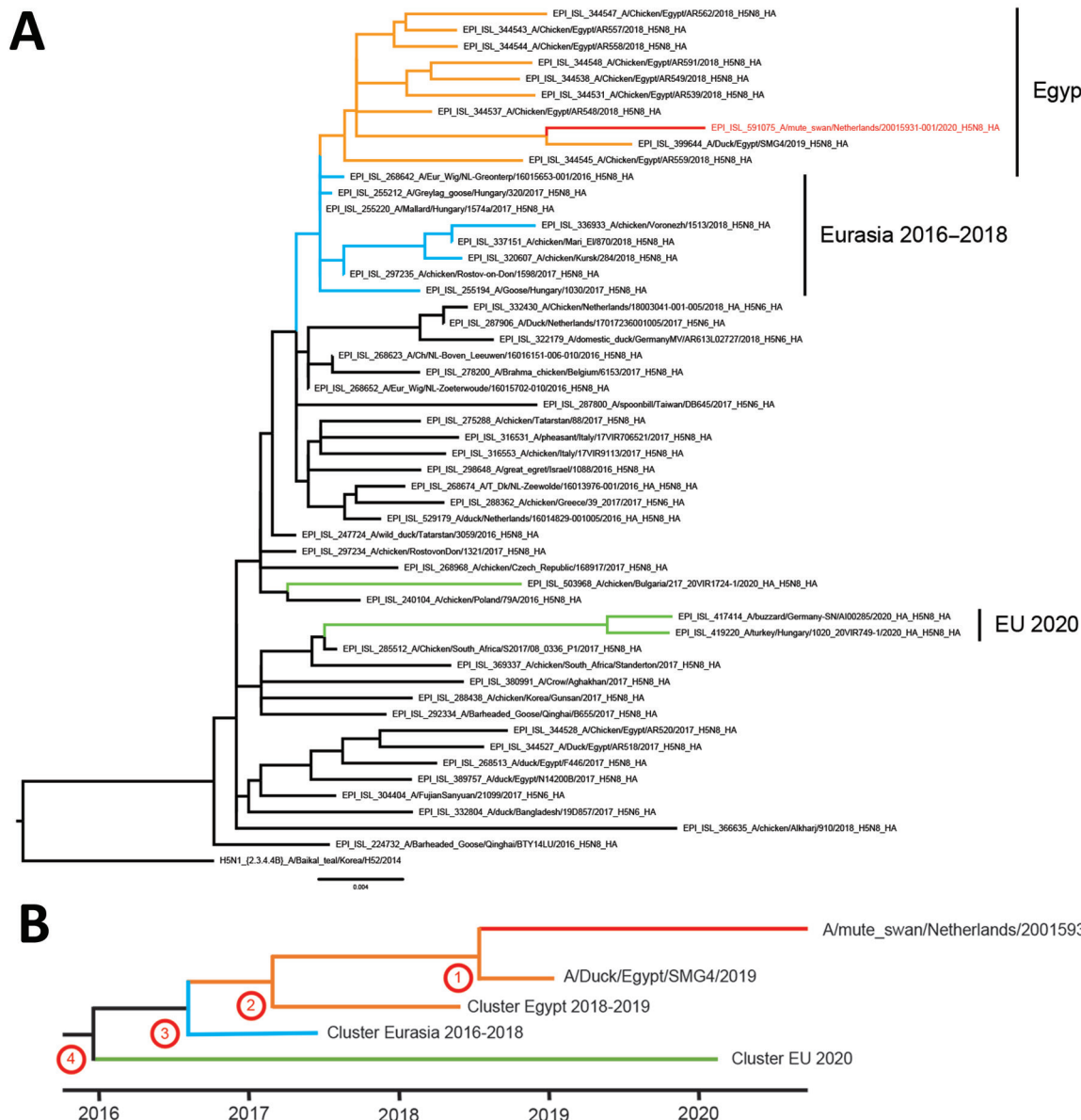


**Figure.** Phylogenetic analysis of the hemagglutinin (HA) segment of highly pathogenic avian influenza A(H5N8) virus, the Netherlands, October 2020. A) Optimal phylogenetic tree was generated by using the maximum-likelihood method (RAxML version 8.2.12; <https://racm-ng.vital>) with 100 bootstrap replicates and is shown and drawn to scale. GISAID (<https://www.gisaid.org>) accession numbers of the viruses are shown in the trees. Scale bar indicates nucleotide substitutions per site. B) Schematic representation of molecular dating of the HA gene segment. The Bayesian coalescent method was used to estimate the time to the most recent common ancestor of the novel H5N8 virus (numbers corresponding to nodes in the Table). Red branches indicate H5N8 virus isolated in the Netherlands in 2020; green, H5N8 viruses isolated in eastern Europe, Germany, and Bulgaria in 2020; orange, viruses detected in Egypt during 2018–2019; and blue, viruses found in Eurasia during 2016–2018. EU, European Union.

**Table.** Calculated tMRCA with 95% HPD and posterior value for highly pathogenic avian influenza A(H5N8) virus, the Netherlands, October 2020\*

Segment	Node†	tMRCA		Height 95% HPD	Posterior value
		Year	Date		
PB2	1	ND	ND	ND	ND
	2	2016.67	Sep 2016	2016.43–2016.88	0.61
	3	2016.47	Jun 2016	2016.20–2016.68	0.97
	4	2012.70	Sep 2012	2010.50–2014.43	0.96
PB1	1	ND	ND	ND	ND
	2	2017.00	Jan 2017	2016.79–2017.14	0.95
	3	2016.56	Jul 2016	2016.35–2016.76	0.94
	4	2011.21	Mar 2011	2007.91–2013.81	1.00
PA	1	ND	ND	ND	ND
	2	2016.67	Sep 2016	2016.44–2016.88	0.01
	3	2016.48	Jun 2016	2016.30–2016.67	1.00
	4	2008.70	Sep 2008	2005.77–2011.20	1.00
HA	1	2018.58	Jul 2018	2018.15–2018.91	1.00
	2	2017.18	Mar 2017	2016.88–2017.44	1.00
	3	2016.62	Aug 2016	2016.46–2016.78	1.00
	4	2015.97	Dec 2015	2015.68–2016.23	0.97
NP	1	ND	ND	ND	ND
	2	2016.89	Nov 2016	2016.52–2017.13	0.87
	3	2016.43	Jun 2016	2016.08–2016.69	1.00
	4	2014.71	Sep 2014	2013.32–2015.77	0.95
NA	1	2018.42	Jun 2018	2017.87–2018.88	1.00
	2	2016.98	Dec 2016	2016.80–2017.12	0.99
	3	2016.71	Sep 2016	2016.51–2016.86	1.00
	4	2016.15	Feb 2016	2015.77–2016.40	1.00
M	A	2016.39	May 2016	2015.84–2016.63	0.19
NS	1	ND	ND	ND	ND
	2	2016.92	Dec 2016	2016.70–2017.03	0.01
	3	2016.48	Jun 2016	2016.00–2016.79	0.96
	4	2015.77	Oct 2015	2014.74–2016.40	1.00

\*HA, hemagglutinin; HPD, highest posterior density interval; M, matrix protein; NA, neuraminidase; ND, not determined; NP, nucleoprotein; NS, nonstructural protein; PA, polymerase acidic; PB1, polymerase basic 1; PB2, polymerase basic 2; tMRCA, median time of the most recent common ancestor.

†Nodes of the time-scaled phylogenetic tree.

We performed full-genome sequencing as described (6) and classified the virus genetically as H5 clade 2.3.4.4b. We performed detailed phylogenetic analyses to study the origin of the novel H5N8 virus (A/mute\_swan/Netherlands/20015931-001/2020, GISAID accession no. EPI591075; <https://www.gisaid.org>). For HA (Figure) and neuraminidase (NA) (Appendix 1 Figure 1, <https://wwwnc.cdc.gov/EID/article/27/6/20-4464-App1.pdf>), the closest genetic relative was isolated from a duck in Egypt during January 2019 (EPI399644; only HA/NA sequences are available). The virus also shares a common ancestor with other viruses detected in Egypt during 2018–2019 and with viruses detected in the Netherlands and Eurasia during 2016–2018. The HA and NA gene segments of the novel H5N8 virus do not cluster with the H5N8 viruses that caused widespread outbreaks in eastern Europe and Germany earlier in 2020 or with viruses detected in Bulgaria during 2020.

For the other gene segments of the novel H5N8 virus, except for the matrix (M) protein segment, clustering was also observed with H5N8 viruses that circulated in Egypt during 2018–2019 and in Eurasia during

2016–2018 (Appendix 1 Figure 1). However, the M segment clusters with HPAI H5N8 viruses isolated in Asia and Egypt in 2016–2018 but also with the viruses found in eastern Europe and Germany during 2020, which suggests that reassortment with those viruses probably occurred for the M segment. No reassortments with low pathogenicity avian influenza viruses were observed for any of the segments. The genetic distance between the novel H5N8 virus and related viruses detected in Egypt and Eurasia appears relatively large, as demonstrated by the long branch lengths in phylogenetic trees (Appendix 1 Figure 1). This finding suggests long-term, undetected circulation of the virus or that intermediate virus sequences were not available in public databases.

We performed molecular dating by using BEAST (10) to estimate the time to the most recent common ancestor (Table; Appendix 1 Figure 2). For the H5 segment, a common ancestor of the novel H5N8 virus and the Egypt 2019 virus (accession no. EPI399644) was dated to July 2018 (node 1; Appendix 1 Figure 2) and with the cluster of viruses from Egypt to approximately March 2017 (node 2; Appendix 1 Figure 2). The common ancestor for the viruses from Eurasia detected during

2016–2018 was dated to August 2016 (node 3; Appendix 1 Figure 2) and with the viruses from eastern Europe and Germany detected in 2020 to approximately December 2015 (node 4; Appendix 1 Figure 2). Similar dating of ancestral viruses was observed for other gene segments, except for M (Appendix 1 Figure 2), for which the common ancestor for the viruses from eastern Europe and Germany detected during 2020 was dated to approximately May 2016 (node A; Appendix 1 Figure 2).

Molecular dating analysis suggests that the ancestor of the novel H5N8 virus detected in the Netherlands during October 2020 has circulated in this genetic form since March 2017 and caused influenza outbreaks in Egypt during 2018–2019. The novel virus incursion is not related to viruses detected in eastern Europe, Germany, and Bulgaria earlier in 2020 but was probably associated with fall migration of wild birds to wintering sites in the Netherlands. Although no HPAI viruses or deaths were observed at wild bird breeding sites in northern Russia, HPAI H5N8 viruses were reported in southern Russia and northern Kazakhstan in September 2020. Some waterfowl species, such as Eurasian wigeon (*Anas penelope*), tufted duck (*Aythya fuligula*), and white-fronted goose (*Anser albifrons*), are known to migrate from these regions to the Netherlands (Dutch Centre For Field Ornithology, <https://vogeltrekatlas.nl/soortzoek2.html>).

The novel virus was first detected in 2 mute swans that do not migrate over long distances. However, a few days later, virus was also detected in a dead Eurasian wigeon, suggesting that this bird species might have been involved in the incursion of the virus into the Netherlands. Because sequences of the viruses detected in Russia and Kazakhstan are unknown, the relationship between these viruses and the virus detected in the Netherlands remains to be determined. During October, wild bird migration is ongoing, and millions of wild birds will reach their wintering sites in Europe in the coming months. This early detection of HPAI H5N8 virus in the Netherlands predicted a high risk for the poultry industry in Europe during the 2020–2021 winter season.

### Acknowledgments

We thank Alex Bossers for providing excellent next-generation sequencing facilities at Wageningen Bioveterinary Research and the authors and submitting laboratories for providing sequences from the GISAID EpiFlu Database (Appendix 2, <https://wwwnc.cdc.gov/EID/article/27/6/20-4464-App2.xlsx>).

This study was supported by the Dutch Ministry of Agriculture, Nature and Food Quality (projects WOT-01-003-087 and KB-37-003-015).

### About the Author

Dr Beerens is a virologist and head of the National Reference Laboratory for Avian Influenza and Newcastle Disease, Lelystad, the Netherlands. Her primary research interests are molecular virology, genetics, and virus evolution.

### References

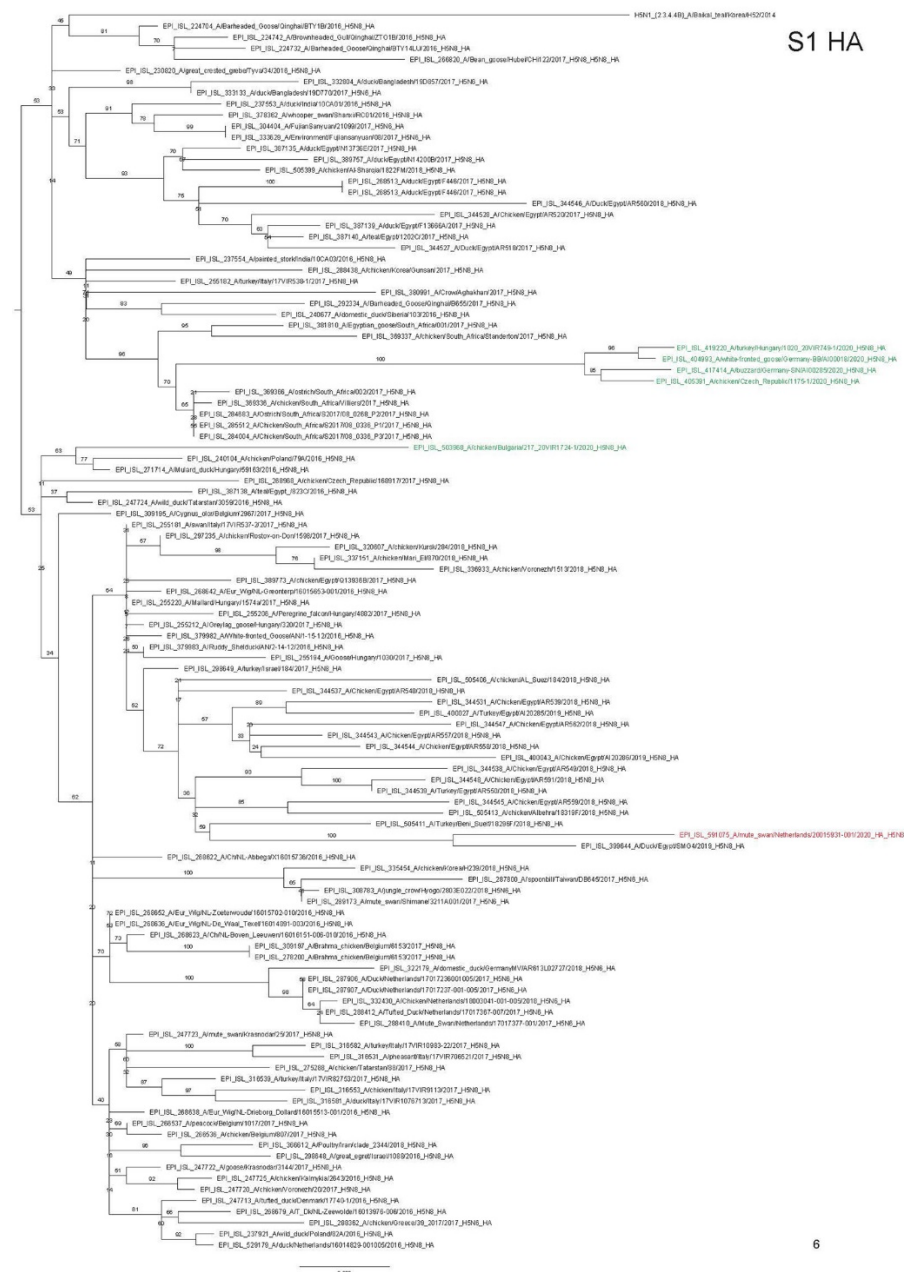
- Gilbert M, Xiao X, Domenech J, Lubroth J, Martin V, Slingenbergh J. Anatidae migration in the western Palearctic and spread of highly pathogenic avian influenza H5N1 virus. *Emerg Infect Dis.* 2006;12:1650–6. <https://doi.org/10.3201/eid1211.060223>
- The Global Consortium for H5N8 and Related Influenza Viruses. Role for migratory wild birds in the global spread of avian influenza H5N8. *Science.* 2016;354:213–7. <https://doi.org/10.1126/science.aaf8852>
- Lee DH, Sharshov K, Swayne DE, Kurskaya O, Sobolev I, Kabilov M, et al. Novel reassortant clade 2.3.4.4 avian influenza A(H5N8) virus in wild aquatic birds, Russia, 2016. *Emerg Infect Dis.* 2017;23:359–60. <https://doi.org/10.3201/eid2302.161252>
- Napp S, Majó N, Sánchez-González R, Vergara-Alert J. Emergence and spread of highly pathogenic avian influenza A(H5N8) in Europe in 2016–2017. *Transbound Emerg Dis.* 2018;65:1217–26. <https://doi.org/10.1111/tbed.12861>
- Lycett SJ, Pohlmann A, Staubach C, Caliendo V, Woolhouse M, Beer M, et al.; Global Consortium for H5N8 and Related Influenza Viruses. Genesis and spread of multiple reassortants during the 2016/2017 H5 avian influenza epidemic in Eurasia. *Proc Natl Acad Sci U S A.* 2020;117:20814–25. <https://doi.org/10.1073/pnas.2001813117>
- Beerens N, Heutink R, Bergervoet SA, Harders F, Bossers A, Koch G. Multiple reassorted viruses as cause of highly pathogenic avian influenza A(H5N8) virus epidemic, the Netherlands, 2016. *Emerg Infect Dis.* 2017;23:1974–81. <https://doi.org/10.3201/eid2312.171062>
- Bergervoet SA, Ho CK, Heutink R, Bossers A, Beerens N. Spread of highly pathogenic avian influenza (HPAI) H5N5 viruses in Europe in 2016–2017 appears related to the timing of reassortment events. *Viruses.* 2019;11:E501. <https://doi.org/10.3390/v11060501>
- King J, Schulze C, Engelhardt A, Hlinak A, Lennermann SL, Rigbers K, et al. Novel HPAIV H5N8 reassortant (clade 2.3.4.4b) detected in Germany. *Viruses.* 2020;12:E281. <https://doi.org/10.3390/v12030281>
- Adlhoch C, Fusaro A, Kuiken T, Niqueux E, Staubach C, Terregino C, et al.; European Food Safety Authority; European Centre for Disease Prevention and Control and European Union Reference Laboratory for Avian Influenza. Avian influenza overview February–May 2020. *EFSA J.* 2020;18:e06194.
- Suchard MA, Lemey P, Baele G, Ayres DL, Drummond AJ, Rambaut A. Bayesian phylogenetic and phylodynamic data integration using BEAST 1.10. *Virus Evol.* 2018;4:vey016. <https://doi.org/10.1093/ve/vey016>

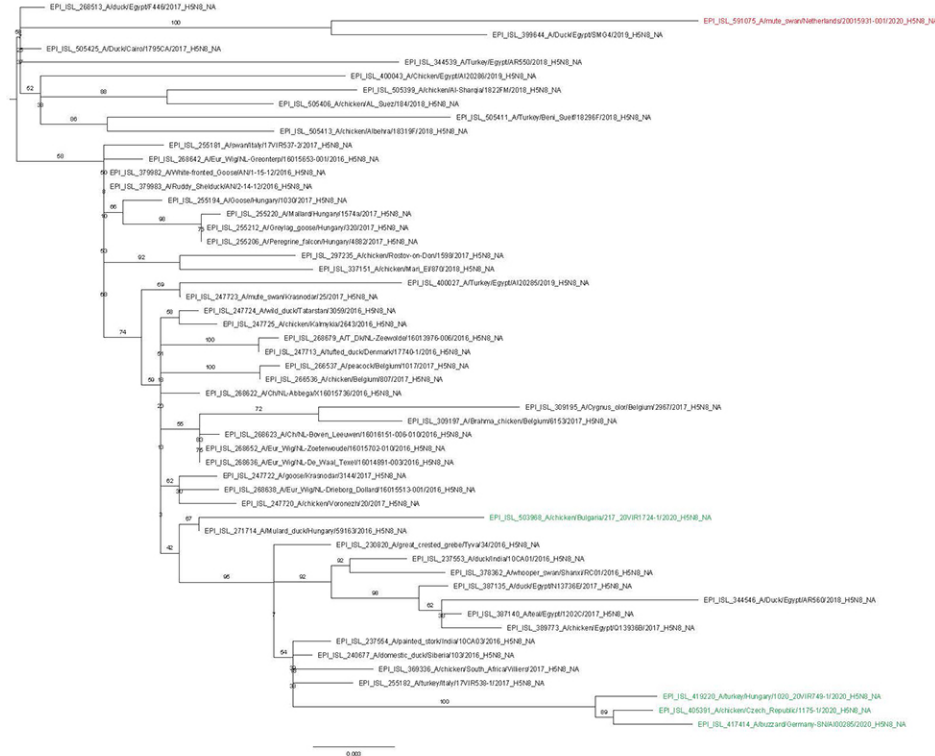
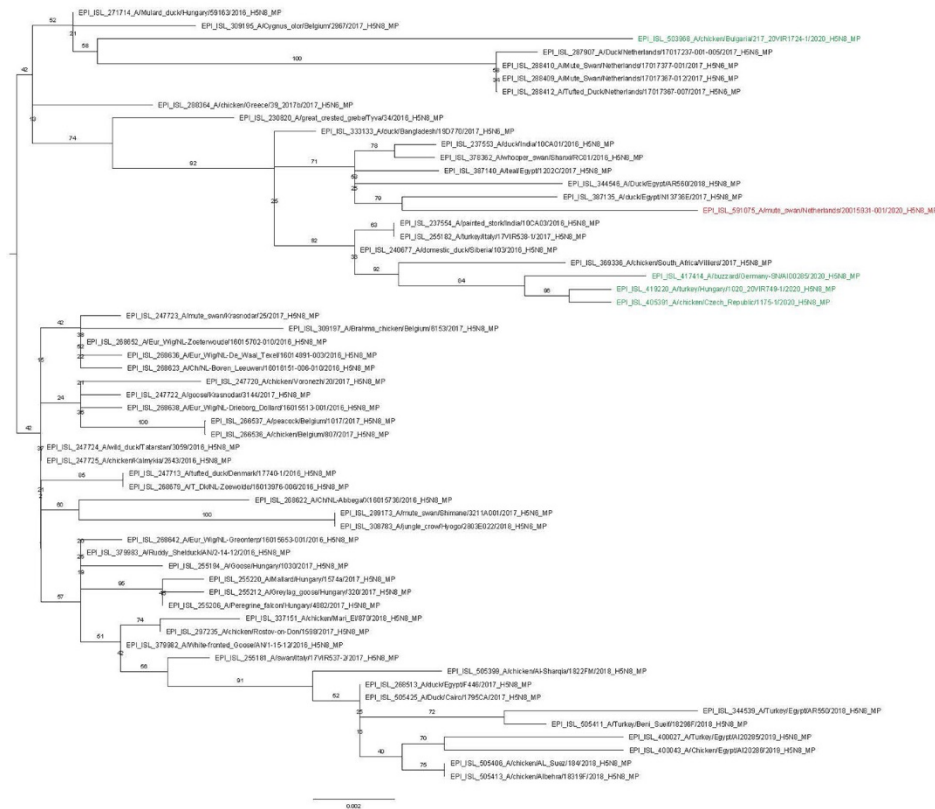
Address for correspondence: Nancy Beerens, Wageningen Bioveterinary Research, Division of Virology, PO Box 65, 8200 AB, Lelystad, the Netherlands; email: [nancy.beerens@wur.nl](mailto:nancy.beerens@wur.nl)

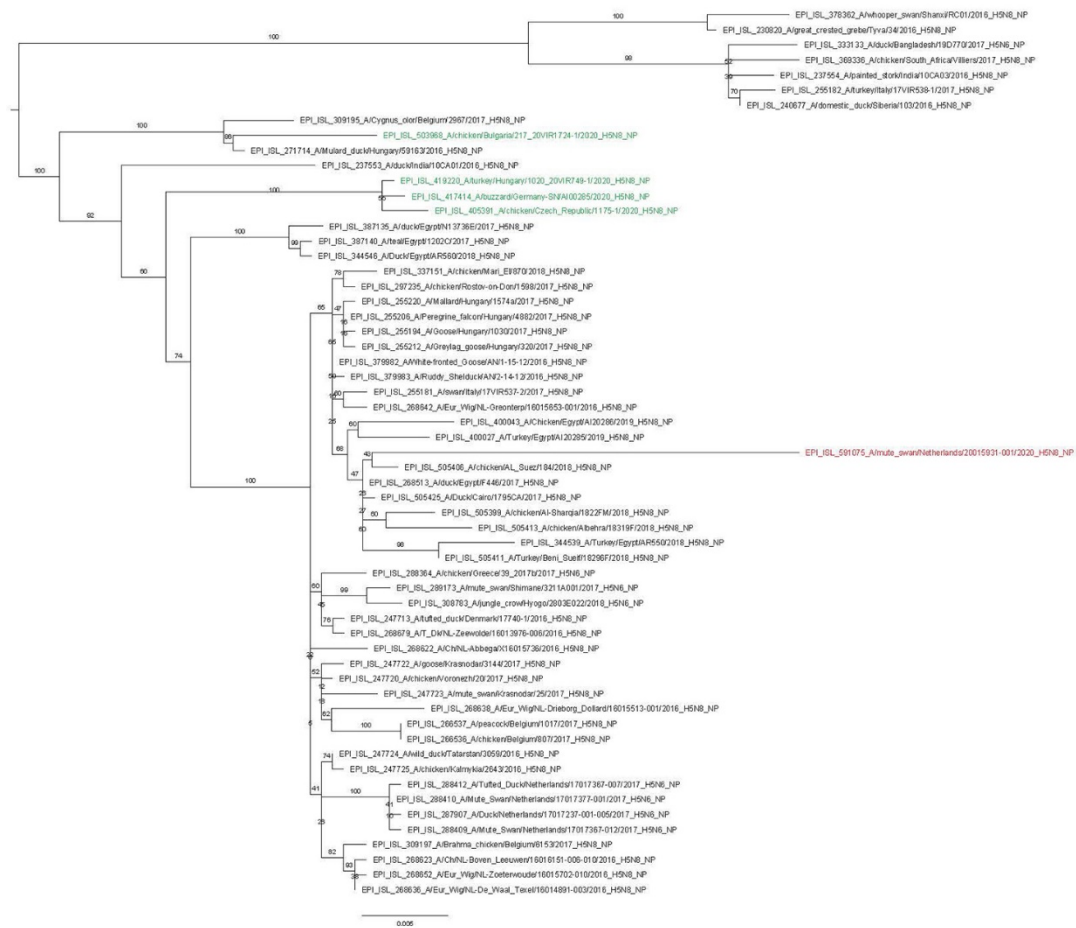


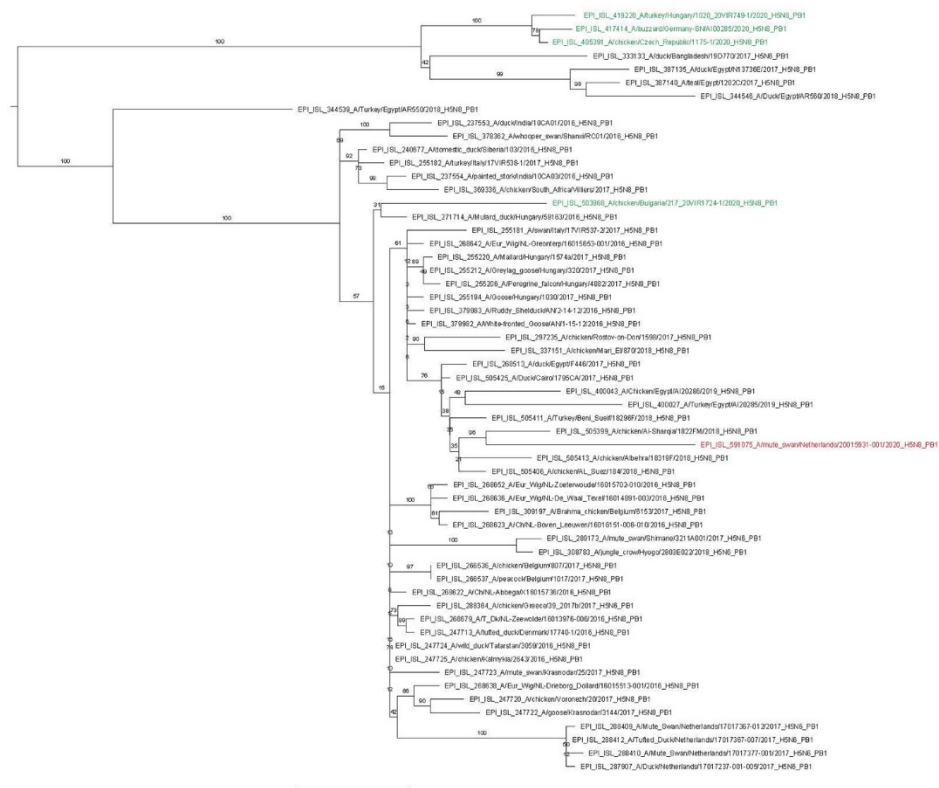
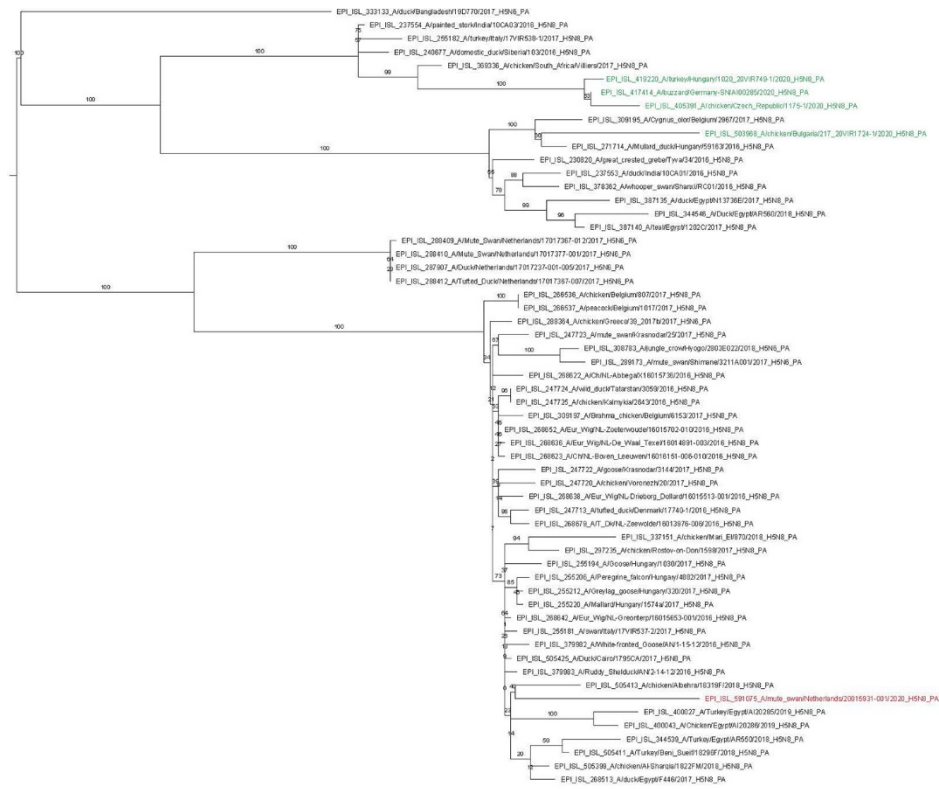
# Incursion of Novel Highly Pathogenic Avian Influenza A(H5N8) Virus, the Netherlands, October 2020

## Appendix

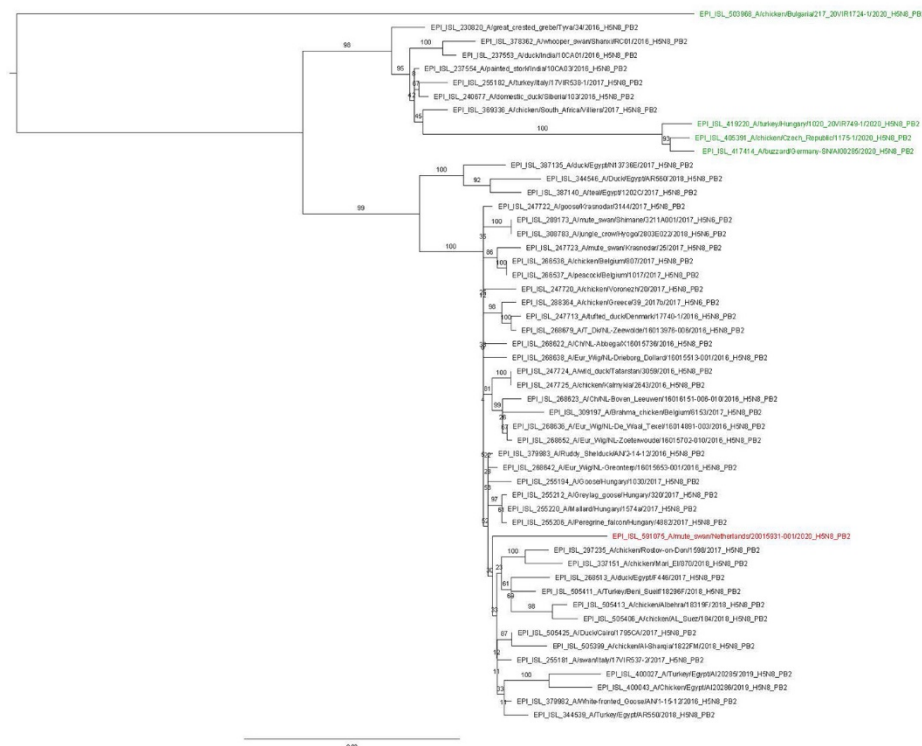




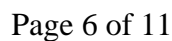






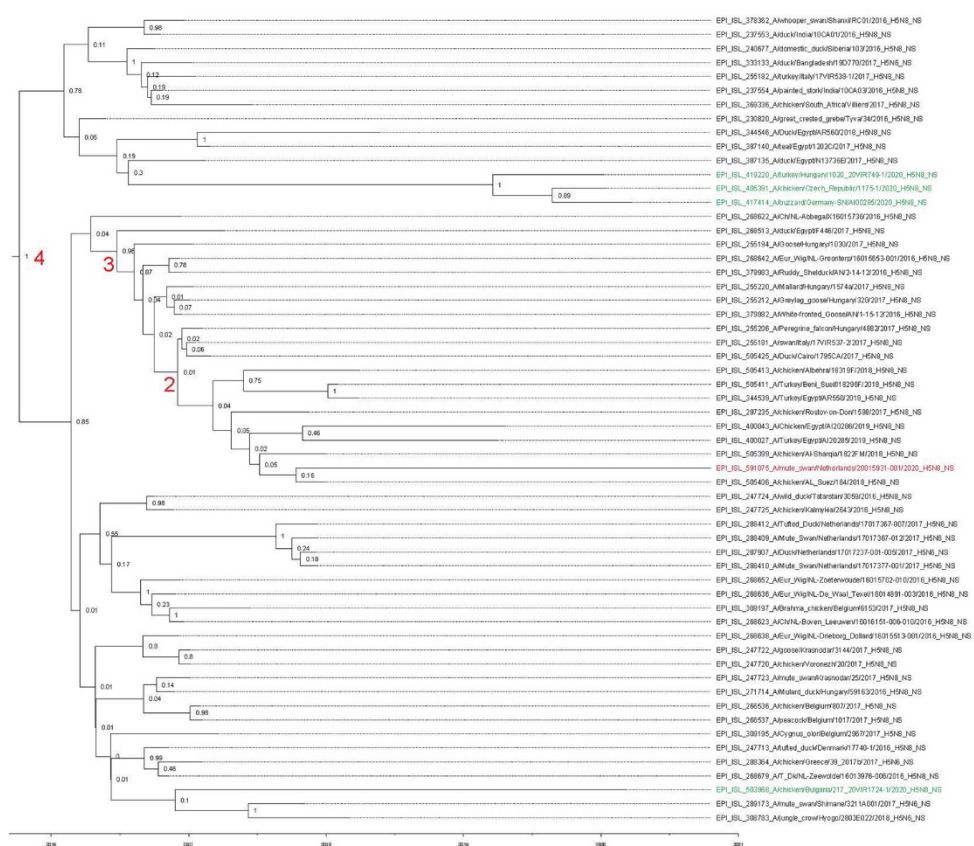


**Appendix Figure 1.** Related sequences were obtained from the GISAID EpiFlu database on October 21, 2020 (<http://www.gisaid.org>) (1) by using a BLAST search. For HA, additional sequences for H5 clade 2.3.4.4b were collected from the EpiFlu database and clustered by using the CD-HIT algorithm (2) and an identity setting of 0.985. Cluster representatives were used in the analysis of HA, in addition to the related sequences from the GISAID BLAST search. Sequences were aligned by using MAFFT v7.427 (3). Maximum-likelihood trees based on the general time-reversible model with a gamma-distributed variation of rates, and 100 bootstraps were generated by using RAXML v8.2.12 (4). The GISAID accession numbers of the viruses are shown in the trees (Appendix Table). The H5N8 virus isolated in the Netherlands in 2020 is marked in red, the H5N8 viruses isolated in Eastern-Europe, Germany and Bulgaria in 2020 are marked in green. Scale bars indicate nucleotide substitutions per site. HA, hemagglutinin; MP, matrix protein; NA, neuraminidase; NP, nucleoprotein; NS, nonstructural protein; PA, polymerase acidic, PB1, polymerase basic 1; PB2, polymerase basic 2.

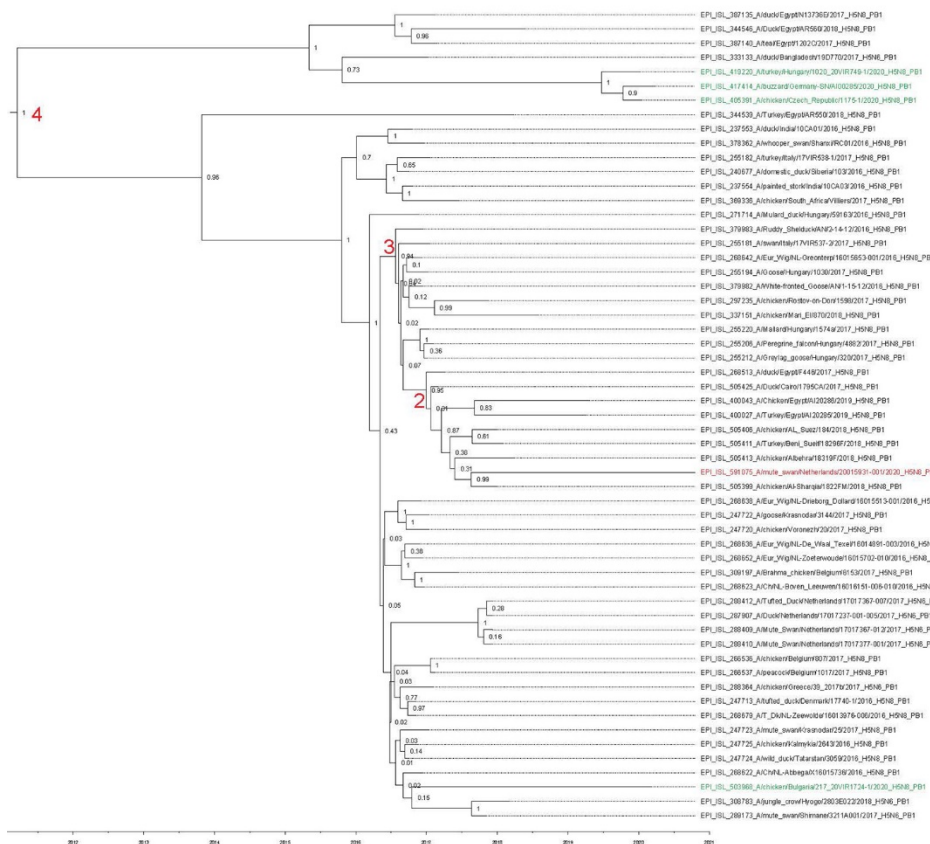


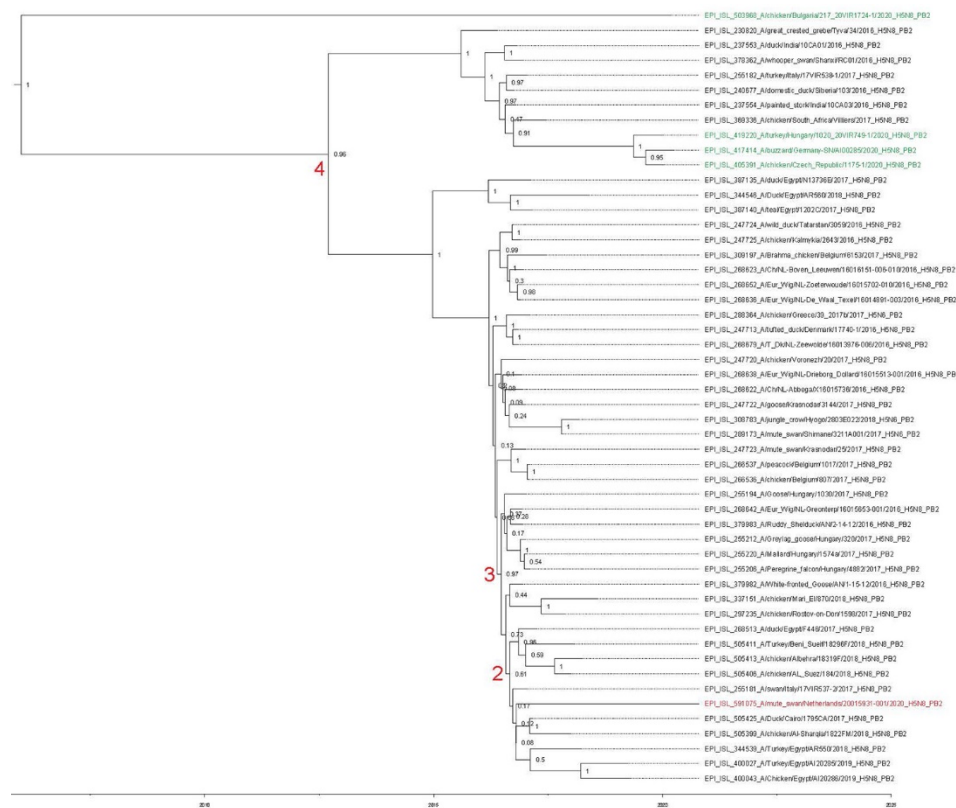












**Appendix Figure 2.** Molecular dating was performed for the all gene segments. Datasets of maximum-likelihood tree analysis (Appendix Figure1) were used for time-scaled phylogenies, which were reconstructed by using a Bayesian Markov chain Monte Carlo framework implemented in the BEAST software package v 1.10.2 (5). Analysis was conducted by using the SRD06 nucleotide substitution model, the Bayesian Skyline coalescent model, and an uncorrelated log normal relaxed molecular clock. Markov chain Monte Carlo runs of  $1 \times 10^8$  states sampling each  $1 \times 10^4$  steps were run to obtain an effective sample size >200. Maximum clade credibility trees were reconstructed with 10% burn-in, and the posterior distribution of relevant parameters were assessed in FigTree v 1.4.4 (6). The time to the most recent common ancestor for the numbered nodes is listed in the Table, as is the credible interval and posterior value. For the MP segment, the letter A was used in this figure and the Table to denote the relationship with the viruses found in eastern Europe and Germany during 2020. Because the MP segment was probably introduced by reassortment, this node is not similar to node 4 for the other segments. GISAID accession numbers are shown in the trees (Appendix Table). H5N8 virus isolated in the Netherlands during 2020 is indicated in red; and viruses isolated in eastern Europe, Germany, and Bulgaria during 2020 are indicated in green. Scale bars indicate time intervals. HA, hemagglutinin; MP, matrix protein; NA, neuraminidase; NP, nucleoprotein; NS, nonstructural protein; PA, polymerase acidic, PB1, polymerase basic 1; PB2, polymerase basic 2; 4, node 4.

## References

1. Shu Y, McCauley J. GISAID: global initiative on sharing all influenza data. *Euro Surveill.* 2017;22:30494.
2. Fu L, Niu B, Zhu Z, Wu S, Li W. CD-HIT: accelerated for clustering the next-generation sequencing data. *Bioinformatics.* 2012;28:3150–2. [PubMed](#) <https://doi.org/10.1093/bioinformatics/bts565>
3. Katoh K, Standley DM. MAFFT multiple sequence alignment software version 7: improvements in performance and usability. *Mol Biol Evol.* 2013;30:772–80. [PubMed](#) <https://doi.org/10.1093/molbev/mst010>
4. Stamatakis A. RAxML version 8: a tool for phylogenetic analysis and post-analysis of large phylogenies. *Bioinformatics.* 2014;30:1312–3. [PubMed](#) <https://doi.org/10.1093/bioinformatics/btu033>
5. Suchard MA, Lemey P, Baele G, Ayres DL, Drummond AJ, Rambaut A. Bayesian phylogenetic and phylodynamic data integration using BEAST 1.10. *Virus Evol.* 2018;4:vey016. [PubMed](#) <https://doi.org/10.1093/ve/vey016>
6. Rambaut A. 2018. FigTree v1.4.4 [cited 2021 Apr 9]. <https://github.com/rambaut/figtree/releases>